ACS OMEGA

Article

Cite This: ACS Omega 2020, 5, 643−649

http://pubs.acs.org/journal/acsodf

Solid-State Chemiresistors from Two-Dimensional MoS_2 Nanosheets Functionalized with L-Cysteine for In-Line Sensing of Part-Per-Billion Cd^{2+} Ions in Drinking Water

Paul Bazylewski,[†,‡] Sheldon Van Middelkoop,[†] Ranjith Divigalpitiya,[‡] and Giovanni Fanchini*[,†,§]

[†]Department of Physics & Astronomy, University of Western Ontario, 1151 Richmond St., London, Ontario N6A 3K7, Canada

[‡]3M Canada Company, 1840 Oxford St., London, Ontario N5V 3R6, Canada

[§]Department of Chemistry, University of Western Ontario, 1151 Richmond Street., London, Ontario N6A 5B7, Canada

Supporting Information

ABSTRACT: Sensing of metal contaminants at ultralow concentrations in aqueous environments is vital in today's overpopulated world, with an extremely stringent limit (<5 ppb) for Cd^{2+} ions in drinking water. Here, we utilize sonochemically exfoliated molybdenum disulfide (MoS_2) nanosheets functionalized with L-cysteine (Cys) as highly sensitive and selective two-dimensional (2D) materials for solid-state chemiresistors. We specifically targeted Cd^{2+} ions due to their high toxicity at low concentrations. MoS_2-Cys nanosheets are fabricated using an ad hoc, low-complexity, one-pot synthesis method. Porous MoS_2−Cys thin films with a high surface area are assembled from these nanosheets. Two-terminal chemiresistors incorporating MoS_2−Cys films are demonstrated to be preferentially sensitive to Cd^{2+} ions at neutral pH, irrespective of other metal ions present in water flowing through the device. A 5 ppb concentration of the Cd^{2+} ions in the water stream increases the device resistivity by 20 times. Our devices operate at broad (1−500 ppb) range and fast (∼1 s) response times. Cd^{2+} is selectively detected because of preferential, size-driven adsorption at the interstitials between L-cysteine functional groups, combined with pH-controlled charge transfer that removes electronic gap states from MoS_2. MoS_2−Cys-based chemiresistors can be deployed in-line to detect metal ions without any need for additional offline measurements.

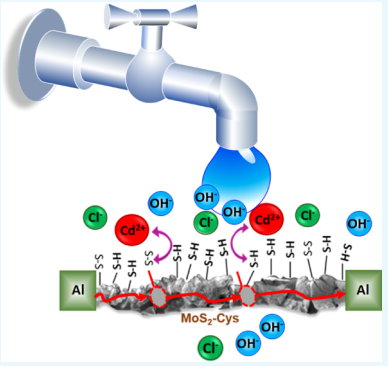

INTRODUCTION

Contamination of global water resources has increased substantially in recent years due to increasing human activity and population. To meet the drinking water requirements of today's world, sophisticated diagnostics of clean water and wastewater streams is vital, especially for concerns of metal-ion contamination.[1] Contaminants commonly found in drinking water include transition metals such as Mn, Fe, Co, Cu, Mo, Zn, Cu, Cd, and Hg, as well as post-transition metals such as Pb, As, and B. All of these contaminants, and others, are globally regulated to levels in the ppb or sub-ppb range.[1] In many cases, metal ions can cause harmful health effects if consumed by humans or animals, which can have acute or chronic consequences due to bioaccumulation. Specifically, the Environmental Protection Agency (EPA) mandated that the limit of Cd in drinking water should be as low as 5 ppb concentration. Comparison of this limit with the significantly higher (50 ppb) EPA limit for manganese, not considered to be damaging to health, is indicative of the importance of high-sensitivity detection of cadmium in water, where it normally restructures as Cd^{2+} ions.

State-of-the-art detection methods for metal ions in water include (i) electrochemical techniques such as anodic stripping voltammetry, which can access the ppb and sub-ppb concentration ranges;[2−9] (ii) optical detection techniques (including fluorescence, luminescence, or colorimetric detection[10−16]) and (iii) electrical transduction sensing via chemiresistor or field-effect transistor architectures.[17−25] Of these detection categories, electrical transduction devices are preferred due to reduced complexity, as they do not require additional offline measurements (such as with optical methods) and are not complicated by the need for high-maintenance cost reference electrodes (as in the case of electrochemical methods).[1] Three-terminal field-effect transistors based on molybdenum disulfide (MoS_2) and diselenide ($MoSe_2$) are known to exhibit high-accuracy and low-detection threshold for gas sensing,[20−27] but equivalent sensors for detection of metal ions in water have not yet been demonstrated. Furthermore, a two-terminal chemiresistor is highly desirable over transistor (triode) architectures in terms of reduced device complexity.

A chemiresistor detects contaminants as they act as dopants or impurities that induce changes in the device's electrical conductivity, even when they are present only at the ppb level.[17−25] This is different from electrochemical sensors in which redox processes must occur at the electrode surface. In

Received: October 1, 2019
Accepted: December 12, 2019
Published: December 26, 2019

DOI: 10.1021/acsomega.9b03246
ACS Omega 2020, 5, 643−649

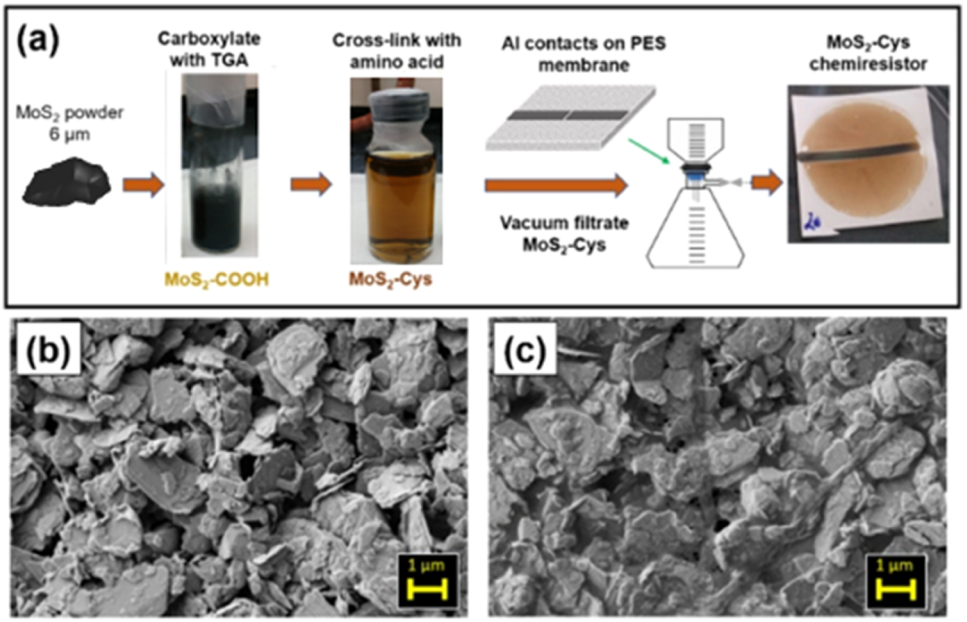

Figure 1. (a) MoS_2−Cys preparation using thioglycolic acid (TGA) to add carboxyl groups followed by amide cross-linking for Cys functionalization and fabrication of two-terminal chemiresistors. MoS_2−Cys thin films can be prepared by vacuum filtration and incorporated in these devices. 2-keV scanning electron microscopy (SEM) images of (b) MoS_2−COOH and (c) MoS_2−Cys (1:20 MoS_2/Cys mass ratio), showing Cys functionalization as a network of filaments on the surface of MoS_2 aggregates. Photographs are the authors' own work.

chemiresistors, thickness and surface area of the active layer are directly related to the sensor response time and sensitivity, with thinner films and higher surface areas leading to better performance. Molybdenum disulfide (MoS_2) is an excellent candidate material for chemiresistor sensing as well as other environmental applications.[28,29] Two-dimensional (2D) MoS_2 nanosheets exhibit p-type semiconducting properties with electrical transport sensitive to doping by charge transfer.[29] Few-layer 2D MoS_2 can be readily exfoliated by solution-processing techniques[28,30] and restacked into thin films by common thin-film fabrication methods, including drop casting, spin coating, and vacuum filtration. Solution-processed MoS_2 nanosheets are uniquely positioned as robust sensing platforms for metal detection because they can be easily decorated with carboxylated groups[28] in a one-pot methodology that favorably compares, in terms of cost competitiveness and low complexity, to the preparation of reduced graphene oxide and epitaxial growth of 2D MoS_2 on graphene or SiC.[18,29] Functionalization of carboxylated MoS_2 (MoS_2−COOH) with amino acids may add receptors that are sensitive to specific metal ions. L-Cysteine and small molecules such as glutathione are known to have a high affinity for divalent metal ions such as Cd and Hg, respectively,[28,31−33] and can be similarly used to sensitize MoS_2 toward these elements.

Here, MoS_2 nanosheets functionalized with L-cysteine (MoS_2−Cys) will be examined as candidate materials for chemiresistors showing high selectivity and preferential sensitivity for Cd^{2+} ions in water at neutral pH in the 1−500 ppb range. These sensors will be prepared from MoS_2−COOH by a simple, low-cost method to display a low detection limit for Cd^{2+}. Chemiresistors based on our technology have been demonstrated to operate irrespective of the presence of counterions or other metal ions in water. Compared to similar devices comprising an active layer of epitaxially grown SiC,[18] MoS_2−Cys will have lower fabrication costs, and will be shown to have a lower detection limit for Cd^{2+}. MoS_2−Cys is anticipated to display selective and tunable sensitivity to different metal ions depending on the pH of the metal ion solution used, where a sensitivity enhancement of 1−2 orders of magnitude can be achieved for Cd^{2+} sensing.

RESULTS AND DISCUSSION

Preparation of our in-line chemiresistor devices utilizes thin films of material deposited on a poly(ether)sulfone (PES) porous support backing to form a high-surface area sensor. The fabrication protocol is summarized in Figure 1a, where the active sensing layer is comprised of MoS_2−Cys. The chemiresistor sensitivity is controlled by defining a sensing area between two metal electrodes, Al in this case, deposited prior to the vacuum filtration of MoS2 solution. Pores in the PES are preserved when the Al thickness is on the order of 100 nm. In this way, both MoS_2−Cys films and Al electrodes are porous and do not disturb the water flow through the device during the sensing process.

Figure 1b,c shows the SEM images of MoS_2-COOH and MoS_2−Cys thin films, respectively. In both panels (b) and (c), it is evident that 2D MoS_2 nanosheets tend to stack in aggregates from 100 nm to 2 μm thickness. Although individual nanoscale platelets are not readily visible by SEM, numerous nanoscale platelets mixed with micron-size pieces have been detected and investigated via atomic force microscopy. The number of layers present in the flakes ranges from 5 to 10 layers for nanoscale platelets to hundreds of layers for micron-size platelets.[28]

Comparison of the two panels demonstrates the effects of cysteine on the thin-film morphology as a cross-linker between MoS_2 platelets. MoS_2−COOH prepared by the same method used here has been previously shown to be mainly arranged in few-layer nanosheets.[28] On the contrary, thicker aggregates are visible in Figure 1b from thin films obtained by vacuum filtration, and a more continuous film is noticeable in panel (c) due to Cys-induced cross-linking. We thus infer that

DOI: 10.1021/acsomega.9b03246
ACS Omega 2020, 5, 643−649

functionalization converts MoS_2−COOH films made of disconnected platelets into cross-linked networks of MoS_2 flakes interconnected by Cys filaments, with the ability to preferentially retain ions with which they exhibit affinity.

Figure 2a presents the SEM micrograph of a MoS_2−Cys chemiresistor channel, along with elemental maps obtained by

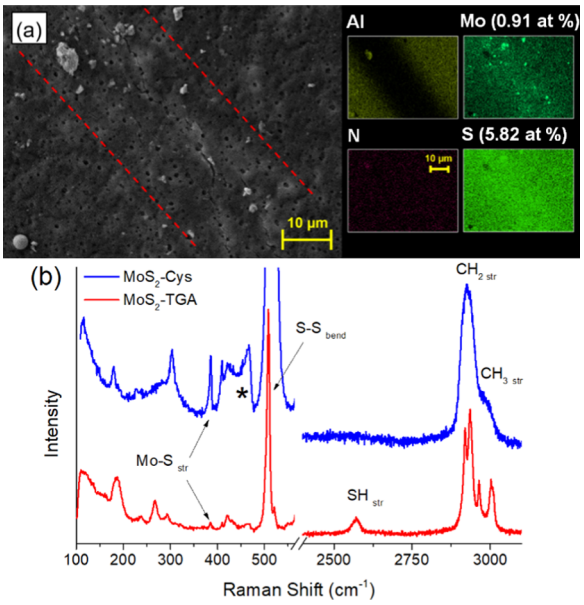

Figure 2. (a) Ten kiloelectron Volts SEM/EDX images of 1:10 mass ratio MoS_2:Cys chemiresistor channel. MoS_2 flakes are visible in the device channel between red dotted lines. Region outside the channel is occupied by Al contacts. The porous nature of the chemiresistor is evidenced by minimally covered 0.8 μm pores (black dots) from the underlying PES membrane. EDX S, Mo, N, and Al maps are also reported. (b) Raman spectra of MoS_2−COOH (blue) and MoS_2−Cys (red) casted on Si wafers. Before Cys functionalization, Raman S−S and SH stretching bands representing residual TGA are clearly visible. After functionalization, a new feature (*) is the fingerprint of Cys attachment to MoS_2.

energy-dispersive X-ray (EDX). Magnification of the SEM image is lower than previously reported in Figure 1b,c. EDX maps show the distribution of N, Mo, and S, as well as Al from the gap-cell contacts. Nitrogen is uniformly distributed, also indicating a uniform presence of Cys filaments, as the only nitrogen source in this system is the amine from these functionals. Mo and S are distributed throughout as expected, with some large particles of MoS_2 visible on the surface. Examination of sulfur atomic percentages determined from EDX show larger amounts of S than expected for stoichiometric MoS_2 alone, confirming that Cys functionals (also containing S) are present.

Figure 2b compares the Raman spectra of MoS_2−COOH and MoS_2−Cys. MoS_2−COOH was measured before being washed to remove unreacted TGA that has not combined with MoS_2. Raman-active S−S bending, S−H stretching, and hydrocarbon stretching modes from TGA are clearly visible, along with the stretching modes characteristic of MoS_2, at 409 and 385 cm^{-1}.[28] After functionalization, the sharp S−H stretching peak of TGA is replaced by a significantly broader counterpart from cysteine, which is centered at ~2650 cm^{-1}. Hydrocarbon modes are also significantly broadened because of the structural disorder introduced by the solid-state nature of these peaks, as opposed to their molecular counterparts in TGA.[28] The most important Raman feature for our work, marked with (*) in Figure 2b, is distinctive of cysteine bonding with the chalcogenide backbone. Assignment of this peak to Cys-bonded MoS_2 has been widely corroborated in ref 28 with additional characterization, which shows a clear upshift of the 409 cm^{-1} Raman peak of MoS_2 in the presence of stable and irreversible L-cysteine functionalization.

We anticipate that stable Cys bonding to MoS_2 is critical toward MoS_2−Cys sensing performance. Figure 3a shows the

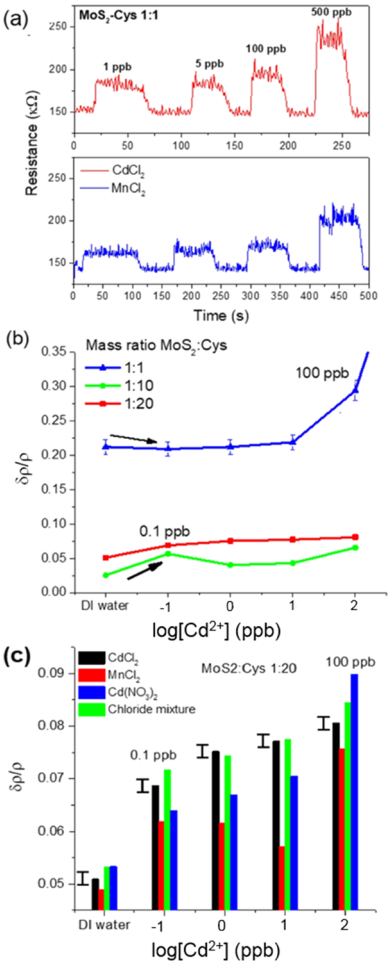

Figure 3. (a) Time domain sensing performance of MoS_2−Cys chemiresistor (MoS_2/Cys = 1:1) for as-prepared $CdCl_2$ and $MnCl_2$ water-containing solutions at 1−500 ppb concentrations. Metal ions are detected by the resulting increase in the resistance ($\delta\rho/\rho$) (b) $\delta\rho/\rho$ of chemiresistors at different MoS_2/Cys mass ratios at different Cd^{2+} concentrations in the presence of Cl^- counterions. (c) $\delta\rho/\rho$ of 1:20 MoS2/Cys chemiresistor challenged with permeation from dilute $CdCl_2$, $Cd(NO3)_2$, and $MnCl_2$, solutions, as well as a 1:1 mixture of $CdCl_2$ and $MnCl_2$. At a very low concentration range, the sensor is selective for Cd^{2+} independent of the counterion present, with the highest sensitivity and lowest interference at 10 ppb.

response of a MoS_2−Cys chemiresistor upon injection with a deionized (DI) water stream contaminated with increasing concentrations of Cd^{2+} ions, from 1 to 500 ppb. The chemiresistors operate by measuring the relative resistivity changes ($\delta\rho/\rho$) over time when impurities are added to water flowing in-line through two-terminal porous MoS_2−Cys gap cells. We anticipate that $\delta\rho$ is normally positive (i.e., MoS_2 resistivity *increases* with increasing metal-ion concentrations in

DOI: 10.1021/acsomega.9b03246
ACS Omega 2020, 5, 643−649

the filtrated water stream). Thus, our sensing process is different from the decrease in water ionic resistance due to impurities.

The response in terms of resistivity increase is nearly immediate (<1 s). However, at MoS_2/Cys = 1:1 mass ratio, differentiation between Mn^{2+} and Cd^{2+} ions is minimal, with both ions appearing to increase the sensor resistance due to charge transfer between MoS_2−Cys and the coordinating metal ions, which remove electronic states (acting as electron donors) from the band gap of MoS_2.[28] Furthermore, the sensitivity of 1:1 mass ratio MoS_2/Cys sensors is below the EPA-mandated level[1] of 5 ppb for Cd in drinking water. Chemiresistor performance reported in Figure 3a needed to be improved both in terms of sensitivity and selectivity, which required to adjust the MoS_2/Cys ratio in the active layer and the pH of the water stream, respectively.

To increase the sensitivity of MoS_2−Cys chemiresistors to lower concentrations of Cd^{2+} ions, larger amounts of L-cysteine were used in the thin-film fabrication process. Figure 3b reports $\delta\rho/\rho$ from chemiresistors prepared from MoS_2−Cys thin films at 1:1, 1:10, and 1:20 MoS_2/Cys mass ratios and their comparison with analytical standards of water at varying concentrations of Cd^{2+} ions. Differently from the 1:1 MoS_2/Cys device, both 1:10 and 1:20 active layers show improved sensitivity to Cd^{2+} due to significantly smaller error bars, which enable a linear response in the 0.1−10 ppb range. However, the price of higher sensitivity to lower concentrations is paid in terms of lower overall magnitude of $\delta\rho/\rho$, as displayed by sensors with a lower MoS_2/Cys ratio. This happens because ρ, the dry base resistance, significantly increases from 140 ± 10 kΩ at 1:1 mass ratio to 250 ± 10 kΩ at 1:20 (see Supporting Information Figure S1). This demonstrates that Cys bonding is a necessary ingredient to improve the electrical conductivity of MoS_2 thin films. As L-cysteine is an electrical insulator, increase in electrical conductivity at higher Cys contents could be assigned to the addition of states in the band gap of MoS_2 via electronic charge transfer.[27]

Consistency of Cd^{2+} sensing performance in the presence of different counterions was also examined. Figure 3c shows the values of $\delta\rho/\rho$ of a 1:20 MoS_2/Cys chemiresistor challenged with (i) Cd^{2+} from $CdCl_2$ and $Cd(NO_3)_2$ (pH = 5.0), (ii) Mn^{2+} (pH = 6.0) from $MnCl_2$ and (iii) a mixture of $CdCl_2$ and $MnCl_2$ (pH = 5.6) leading to interference of Mn^{2+} and Cd^{2+} ions. At the lowest concentrations, this chemiresistor is preferentially selective to Cd^{2+}, with the highest sensitivity and lowest interference observed at 10 ppb. For a single ion−counterion pair, the sensors shown here are capable of quantitatively indicating the concentration in the 1−100 ppb range. When a mixture with different counterions is used, the sensors continue to function qualitatively to determine if Cd is present at very low concentrations, but the observed difference between Cd concentration values decreases, making the concentration more difficult to determine. This effect results from the sensitivity to different ions at different concentrations depending on the MoS_2/Cys ratio used in the fabrication process. However, because of the strong difference in the acidity of the water streams used in Figure 3c, detailed understanding of the optimal performance in terms of pH is required.

To examine the effect of pH on the chemiresistor performance, 10 ppb solutions of Cd^{2+} and Mn^{2+} ions were tested at buffered pH from 3 to 10. Figure 4a shows $\delta\rho/\rho$ for 1:20 MoS_2/Cys sensors at varying pH. At the lowest (pH < 5)

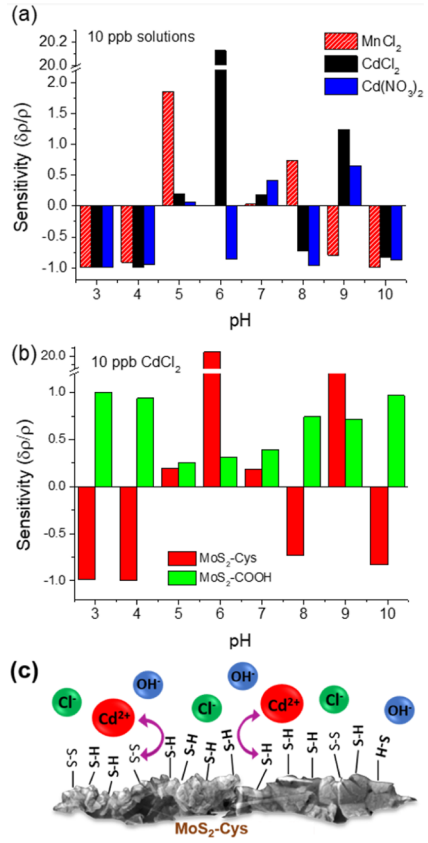

Figure 4. Bar graphs demonstrating the sensitivity of (a) MoS_2−Cys sensors to different metal ions depending on the pH and metal ion used and (b) MoS_2−COOH compared to MoS_2−Cys using a 10 ppb solution at varying pH. (c) Charge transfer at the nanostructured surface of MoS_2−Cys films. The high surface area facilitates charge transfer between dilute metal ions and the thiol and disulfide groups that modulate the conductivity across the MoS_2 backbone of the chemiresistor.

and highest (pH > 9) values, little selectivity can be noticed between metal ions at similar hydrodynamic radii, such as Cd^{2+} and Mn^{2+}. Chemiresistors are "shorted" by the high ionic conductivity of water, with low resistances in the 10−1000 Ω range (Figure 2S, Supporting Information). This limits the useful sensing window to pH = 5−9, which is well within the range for drinking water. Selectivity to different ions still varies dramatically in this range. However, at a neutral pH of 6−7 (i.e., the values expected for drinking water), Figure 4a also shows that the sensor is highly sensitive to Cd^{2+} regardless of the presence of chloride or nitrate counterions. Interference from Mn^{2+} ions is also negligible in this range by comparison. This indicates that optimized MoS_2−Cys chemiresistors fabricated at 1:20 constituent ratios satisfy the detection requirements for Cd^{2+} ions, both in terms of sensitivity and selectivity from metal ions of comparable radii. Of course, additional selectivity from metal ions at different hydrodynamic radii can always be obtained by preliminary filtration of the water stream.

From a fundamental standpoint, it is worth noting that sensing of Cd^{2+} is also enhanced at pH = 9.0 due to the formation of $Cd(OH)_2$ groups that may form in basic environments. The formation of these groups is independent of the counterions present, and our results indicate that MoS_2−Cys chemiresistors are strongly sensitive to them.

DOI: 10.1021/acsomega.9b03246
ACS Omega 2020, 5, 643−649

Although Cd^{2+} sensing is dramatically enhanced at pH = 9, this effect is completely overshadowed by the tremendous sensitivity increase (~20) at neutral pH. At this pH level, $CdCl^+$ complexes are present, as Cd is not completely dissociated from Cl ions. MoS_2−Cys is found to be uniquely sensitive to this compound, perhaps due strong interaction with S−H and S−S ligands present on cysteine and cystine in the MoS_2−Cys layer. Additionally, at this pH level, the sensor shows a very strong but negative (i.e., $\delta\rho < 0$) sensitivity for $Cd(NO_3)_2$, allowing for not only selectivity for Cd^{2+} at the appropriate pH but also for the type of counterion present in this specific case. While MoS_2−Cys provides minimal sensitivity to Mn at neutral pH, Figure 2a shows that sensitivity to Mn^{2+} can be obtained at different pH windows, and specifically at pH = 5 and 8 when $MnCl_2$ and $MnOH^+$ complexes are present, respectively. These results indicate that MoS_2−Cys chemiresistors can be modified to detect different metal ions by modifying the pH of the water stream.

To investigate the role of cysteine in the sensing mechanism, chemiresistors from MoS_2−COOH were also constructed, and their performance is shown in Figure 2b under the same testing conditions as that of the MoS_2−Cys device in panel (a). It can be readily observed that, at pH = 6−7, $\delta\rho/\rho \approx 0.3$ for the MoS_2−COOH device, to be compared with $\delta\rho/\rho \approx 20$ for MoS_2−Cys. We thus infer that sensitivity to Cd^{2+} ions is clearly due to cysteine and is not a native property of MoS_2. Furthermore, although MoS_2−COOH appears to be sensitive to Cd^{2+}, $\delta\rho/\rho$ has been found to be independent of the specific metal ion in such chemiresistors and is a sole consequence of changes in pH. This can also be inferred from the approximately linear increase in $\delta\rho/\rho$ from pH = 5 to 10. Along with the morphology noticeable from Figure 2b,c, this result strongly suggests that preferential sensitivity of MoS_2−Cys to Cd^{2+} is not the result of metal-ion intercalation between MoS_2 layers but due to Cd^{2+} adsorption at cysteine functionals, which modifies the charge transfer processes between cysteine-based functional groups and the MoS_2 backbone. As shown in Figure 4c, the high surface area and thinness of the MoS_2−Cys film facilitates charge transfer between the metal ions and solution over a large area, which is sufficient to affect the conductivity of the film backbone, even at very dilute ion concentrations in water. Electrical transport in solids is extremely sensitive to the presence of gap states. We thus suspect that Cd^{2+} is selectively detected because of its size-driven affinity to L-cysteine, combined with charge transfer that removes electronic states from the electronic band gap of MoS_2. The degree of charge transfer depends on the number and type of ions present in the solution and can be increased or decreased by tuning the pH of the incoming solution.

CONCLUSIONS

MoS_2−Cys thin films have been shown to sense dilute Cd^{2+} ions in water at neutral pH and in the 1−10 ppb range, with high selectivity and low interference from other metal ions. MoS_2−Cys porous chemiresistors are shown to have tunable sensitivity to different metal ions depending on the pH of filtrated water. Cd^{2+} is preferentially adsorbed by the Cys groups (consistently with significantly lower effects in MoS_2−COOH), and ions are sensed through charge transfer at the surface of MoS_2−Cys films with a high density of thiol and disulfide groups that modulate their conductivity. MoS_2−Cys is a chemiresistor that can be easily produced in large quantities using readily available raw materials and low-complexity fabrication methods. The chemiresistive devices described in this paper are naturally porous and permeated by water, so they can be used to provide in-line and real-time sensing information about metal-ion concentration, with high reusability. Their response time is ~1 s, or less. The lower detection limit is in the sub-ppb range, and sensing can be accomplished without any need for offline measurements or additional equipment, as in the case of electrochemical or optical detection methods. Our work provides a benchmark for chemiresistor design using functionalized MoS_2 to sense metal ions in water.

MATERIALS AND METHODS

Preparation of MoS_2−Cys Suspensions. A detailed description of the methodology used for the preparation of MoS_2−Cys is reported by Bazylewski et al.[28,31] Briefly, 7.6 g of microcrystalline MoS_2 powder (Sigma Aldrich, CAS 1317-33-5; 6 μm average grain size, 40 μm grain size max) was mixed with 38 mL of thioglycolic acid (TGA, Sigma Aldrich, CAS 68-11-1) and stirred for 24 h at room temperature. Four hundred milliliters of distilled water was added to the mixture that was ultrasonicated for 2 h to produce a stable suspension of carboxylated MoS_2 (MoS_2−COOH) nanosheets at 1.5 g/L concentration. Functionalization with L-cysteine (Sigma Aldrich, CAS 59-90-4) was performed by amide cross-linking. To this end, *N*-(3-dimethyl-aminopropyl)-*N*′-ethylcarbodiimide hydrochloride (EDC, Sigma Aldrich, CAS 25952-53-8) and *N*-hydroxy-succinimide (NHS, Sigma Aldrich, CAS 6066-82-6) were added to the suspension at 1:1 and 1:1.5 (respectively) mass ratios over MoS_2 and stirred for 15 min. Afterward, MoS_2/Cys is obtained by mixing an L-cysteine solution in distilled water to these suspensions.[28,31] L-Cysteine solutions can be prepared at varying Cys concentrations to adjust the MoS_2/Cys mass ratio at the desired level, where MoS_2/Cys mass ratios of 1:20 or less have been found to remain stable in water over periods longer than one month. Specific characterization protocols are used to determine the cysteine bonding regime in MoS_2−Cys.[28]

Chemiresistor Fabrication and Measurement. Thin films of MoS2−Cys were prepared from 50 mL of solution deposited on poly(ether)sulfone (PES, 3M Co.) membranes with 0.8 μm pore size accordingly to the vacuum filtration method originally developed by Eda et al.[34] for graphene oxide thin films. These films are subsequently dried in air for 4 h at room temperature prior to further processing. A gap cell consisting of two aluminum electrodes (1 mm width, 100 nm thickness, 25 μm gap between) was evaporated on these films at base pressures better than 10^{-6} mTorr in a Kurt−Lesker thermal evaporator setup, with the Al thickness measured in situ by a Sycom STM-2 quartz crystal monitor. Electrodes are defined using a shadow mask.

Chemiresistor fabrication was completed by integrating the two-terminal gap cell described above into a custom-built transducing apparatus reported in detail by Van Middelkoop et al.[35] In this setup, Al electrodes are contacted with a bridge circuit interfaced with a digital−analog converter (Emant 300) that is computer-controlled by a Matlab routine for continuous monitoring of the device resistivity over time. This apparatus includes a 100 mL capacity funnel on top of the Al/MoS_2−Cys/PES gap cell membrane and a fritted glass support connected to a pump underneath. Initially, the device resistivity is primed by filtrating 100 mL of high-resistivity (18 MΩ cm) deionized (DI) water through the porous

DOI: 10.1021/acsomega.9b03246
ACS Omega 2020, 5, 643−649

chemiresistor, during which baseline resistivity (ρ) is measured by applying, at each time interval, an array of currents in the 0−600 μA range at a 40 μA step. Resulting voltages are measured, and ρ is determined through the slope of the $I-V$ curves. As this is significantly lower than water resistivity, ρ is proportional the resistance of the MoS_2−Cys gap cell.

Tests were performed by adding to 5−8 mL of water with dissolved metal ions into the 100 mL DI water funnel, while $\delta\rho$ is continuously monitored by the transducing circuit of the chemiresistor. In a variety of tests, calibrated water solutions at metal ion concentrations from 0.1 to 500 ppb were poured through the apparatus. Addition of ion-containing water to the filtration stream is repeated with high reproducibility and low $\delta\rho/\rho$ drift over time. Metal-containing solutions were prepared using $CdCl_2$ (Sigma Aldrich, CAS 10108-64-2) and $Cd(NO_3)_2{\cdot}4H_2O$ (CAS 10022-68-1) measured by a high-accuracy Denver PI314 scale and dissolved in deionized water by considering the concentration of metal ions (either Mn^{2+} or Cd^{2+}) in the range of 0.1−500 ppb. Preferential sensitivity to Cd^{2+} is verified in the presence of different counterions (i.e., Cl^- and NO_3^-, from $CdCl_2$ and $Cd(NO_3)_2{\cdot}4H_2O$, respectively) and with metal ions (e.g., Mn^{2-}) at similar hydrodynamic radius as that of Cd^{2+}. Control experiments with MoS_2−COOH active layers in lieu of MoS_2−Cys have also been performed. Throughout the course of standard testing, each sensor (of 0.025^2 mm size over a 25 mm^2 filtration disk) is primed with a minimum of 10 L of water passed through it before metal contaminants are tested.

Thin Film Microscopic Characterization. A Zeiss scanning electron microscope (LEO 1540XB) equipped with an energy-dispersive X-ray (EDX) spectrometer with imaging capabilities was used to characterize MoS_2−COOH and MoS_2−Cys thin films and map the distribution of Mo and S (from MoS_2) and N (from Cys). SEM samples were prepared by vacuum filtration onto polycarbonate membranes (pore size 0.5 μm). Samples were coated with 1 nm layer of osmium prior to measurement to increase the surface conductivity using an Os plasma coater (Flogen, OPC80T). Samples of sensor devices for EDX analysis were measured as prepared, on PES membranes. Extensive additional structural and spectroscopic characterization is reported elsewhere.[28,31]

Raman Characterization. Unpolarized Raman spectra were recorded on a Renishaw InVia microspectrometer in a backscattering arrangement. A 633 nm helium−neon laser with a maximum output power of 17 mW was used as the excitation source. The power at the sample surface was 0.02 mW/μm^2 across an 8 μm^2 area. Special attention was paid to avoid damage of the sample by heating by shuttering the laser when not actively measuring. Raman measurements were performed on MoS_2−COOH and MoS_2−Cys samples cast from solution onto (110) silicon wafers. Samples were dried at 50 °C in air, then washed with distilled water, and dried again at 50 °C for 30 min.

■ ASSOCIATED CONTENT

Supporting Information

The Supporting Information is available free of charge at https://pubs.acs.org/doi/10.1021/acsomega.9b03246.

Additional graphics and tables on baseline resistances and performance of MoS_2 chemiresistors (PDF)

■ AUTHOR INFORMATION

Corresponding Author

*E-mail: gfanchin@uwo.ca.

ORCID

Giovanni Fanchini: 0000-0002-2502-7475

Author Contributions

The manuscript was written through contributions of all the authors. All the authors have given approval to the final version of the manuscript.

Notes

The authors declare no competing financial interest.

■ ACKNOWLEDGMENTS

P.B. acknowledges an Ontario Centres of Excellence (OCE) Talent Edge Postdoctoral Fellowship. G.F. acknowledges a Canada Research Chair in Carbon-based nanomaterials and Nano-optoelectronics. Funding from the Canada Foundation for Innovation (award no. 212442) and the Discovery Grant program of the Natural Sciences and Engineering Research Council of Canada (RGPIN-2015-06004) are also gratefully acknowledged. Part of this work was carried out at the Western University Nanofabrication Facility.

■ REFERENCES

(1) Kruse, P. Review on water quality sensors. *J. Phys. D: Appl. Phys.* **2018**, *51*, No. 203002.

(2) Zhao, D.; Guo, X.; Wang, T.; Alvarez, N. T.; Shanov, V. N.; Heineman, W. R. Simultaneous Detection of Heavy Metals by Anodic Stripping Voltammetry Using Carbon Nanotube Thread. *Electroanalysis* **2014**, *26*, 488−496.

(3) Gao, W.; Nyein, H. H. Y.; Shahpa, Z.; Fahad, H. M.; Chen, K.; Emaminejad, S.; Gao, Y.; Tai, L.-C.; Ota, H.; Wu, E.; Bullock, J.; Zeng, Y.; Lien, D.-H.; Javey, A. Wearable Microsensor Array for Multiplexed Heavy Metal Monitoring of Body Fluids. *ACS Sens.* **2016**, *1*, 866−874.

(4) Ruecha, N.; Rodthongkum, N.; Cate, D. M.; Volckens, J.; Chailapakul, O.; Henry, C. S. Sensitive electrochemical sensor using a graphene-polyaniline nanocomposite for simultaneous detection of Zn(II), Cd(II), and Pb(II). *Anal. Chim. Acta* **2015**, *874*, 40−48.

(5) Kang, W.; Pei, X.; Rusinek, C. A.; Bange, A.; Haynes, E. N.; Heineman, W. R.; Papautsky, I. Determination of Lead with a Copper-Based Electrochemical Sensor. *Anal. Chem.* **2017**, *89*, 3345−3352.

(6) Xuan, X.; Park, J. Y. A miniaturized and flexible cadmium and lead ion detection sensor based on micro-patterned reduced graphene oxide/carbon nanotube/bismuth composite electrodes. *Sens. Actuators, B* **2018**, *255*, 1220−1227.

(7) Simpson, A.; Pandey, R. R.; Chusuei, C. C.; Ghosh, K.; Patel, R.; Wanekaya, A. K. Fabrication characterization and potential applications of carbon nanoparticles in the detection of heavy metal ions in aqueous media. *Carbon* **2018**, *127*, 122−130.

(8) Abdul, W.; Muhammad, M.; Nisar, U. Periodic-Table-Style Paper Device for Monitoring Heavy Metals in Water. *Trends Anal. Chem.* **2018**, *105*, 37−51.

(9) Li, L.; Liu, D.; Shi, A.; You, T. Simultaneous stripping determination of cadmium and lead ions based on the N-doped carbon quantum dots-graphene oxide hybrid. *Sens. Actuators, B* **2018**, *255*, 1762−1770.

(10) Zhang, L.; Huang, X.; Cao, Y.; Xin, Y.; Ding, L. Fluorescent binary ensemble based on pyrene derivative and sodium dodecyl sulfate assemblies as a chemical tongue for discriminating metal ions and brand water. *ACS Sens.* **2017**, *2*, 1821−1830.

(11) Liu, S.; Qin, X.; Tian, J.; Wang, L.; Sun, X. Photochemical preparation of fluorescent 2,3-diaminophenazine nanoparticles for

DOI: 10.1021/acsomega.9b03246
ACS Omega 2020, 5, 643−649

sensitive and selective detection of Hg(II) ions. *Sens. Actuators, B* **2012**, *171*−*172*, 886−890.
(12) Ullah, N.; Mansha, M.; Khan, I.; Qurashi, A. Nanomaterial-based optical chemical sensors for the detection of heavy metals in water. *Trends Anal. Chem.* **2018**, *100*, 155−166.
(13) Rana, M.; Chowdhury, P. L-glutathione capped CdSeS/ZnS quantum dot sensor for the detection of environmentally hazardous metal ions. *J. Lumin.* **2019**, *206*, 105−112.
(14) Kim, S.; Gwon, S.; Bae, J. A highly selective ratiometric chemosensor for Hg^{2+} based on 1,2-diaminoanthraquinone. *Sen'i Gakkaishi* **2014**, *70*, 254−257.
(15) Sasaki, Y.; Minamiki, T.; Tokito, S.; Minami, T. A molecular self-assembled colourimetric chemosensor array for simultaneous detection of metal ions in water. *Chem. Commun.* **2017**, *53*, 6561−6564.
(16) Sareen, D.; Kaur, P.; Singh, K. Strategies in detection of metal ions using dyes. *Coord. Chem. Rev.* **2014**, *265*, 125−154.
(17) Gong, J.-L.; Sarkar, T.; Badhulika, S.; Mulchandani, A. Label-free chemiresistive biosensor for mercury (II) based on single-walled carbon nanotubes and structure-switching DNA. *Appl. Phys. Lett.* **2013**, *102*, No. 013701.
(18) Santangelo, M. F.; Shtepliuk, I.; Filippini, D.; Ivanov, I. G.; Yakimova, R.; Eriksson, J. Real-time sensing of lead with epitaxial graphene-integrated microfluidic devices. *Sens. Actuators, B* **2019**, *288*, 425−431.
(19) Varghese, S. S.; Varghese, S. H.; Swaminathan, S.; Singh, K. K.; Mittal, V. Two-dimensional materials for sensing: graphene and beyond. *Electronics* **2015**, *4*, 651−687.
(20) Late, D. J.; Doneux, T.; Bougouma, M. Single-layer MoSe2 based NH3 gas sensor. *Appl. Phys. Lett.* **2014**, *105*, No. 233103.
(21) He, Q.; Zeng, Z.; Yin, Z.; Li, H.; Wu, S.; Huang, X.; Zhang, H. Fabrication of Flexible MoS2 Thin-Film Transistor Arrays for Practical Gas-Sensing Applications. *Small* **2012**, *8*, 2994−2999.
(22) Li, H.; Yin, Z.; He, Q.; Li, H.; Huang, X.; Lu, G.; Fam, D. W. H.; Tok, A. L. Y.; Zhang, Q.; Zhang, H. Fabrication of Single- and Multilayer MoS2 Film-Based Field-Effect Transistors for Sensing NO at Room Temperature. *Small* **2012**, *8*, 63−67.
(23) Perkins, F. K.; Friedman, A. L.; Cobas, E.; Campbell, P. M.; Jernigan, G.; Jonker, B. T. Chemical Vapor Sensing with Monolayer MoS_2. *Nano Lett.* **2013**, *13*, 668−673.
(24) Late, D. J.; Huang, Y.-K.; Liu, B.; Acharya, J.; Shirodkar, S. N.; Luo, J.; Yan, A.; Charles, D.; Waghmare, U. V.; Dravid, V. P.; Rao, C. N. R. Sensing Behavior of Atomically Thin-Layered MoS_2 Transistors. *ACS Nano* **2013**, *7*, 4879−4891.
(25) Liu, B.; Chen, L.; Liu, G.; Abbas, A. N.; Fathi, M.; Zhou, C. *ACS Nano* **2014**, *8*, 5304−5314.
(26) Saravanan, A.; Huang, B.-R.; Chu, J. P.; Prasannan, A.; Tsai, H.-C. High-Performance Chemical Sensing Using Schottky-Contacted Chemical Vapor Deposition Grown Monolayer MoS2 Transistors. *Sens. Actuators, B* **2019**, *292*, 70−79.
(27) Wang, Z.; Mi, B. Environmental Applications of 2D Molybdenum Disulfide Nanosheets. *Environ. Sci. Technol.* **2017**, *51*, 8229−8244.
(28) Bazylewski, P.; Van Middelkoop, S.; Divigalpitiya, R.; Fanchini, G. Few-layer molybdenum disulfide nanosheets functionalized with l-cysteine for selective capture of Cd2+ ions. *Flat Chem.* **2018**, *11*, 15−23.
(29) Santhana Krishna Kumar, A.; Jiang, S.-J. Preparation and characterization of exfoliated graphene oxide−L-cystine as an effective adsorbent of Hg (II) adsorption. *RSC Adv.* **2015**, *5*, 6294.
(30) Ries, L.; Petit, E.; Michel, T.; Diogo, C. C.; Gervais, C.; Salameh, C.; Behelany, M.; Balme, S.; Miele, P.; Onofrio, N.; Voiry, D. Enhanced sieving from exfoliated MoS2 membranes via covalent functionalization. *Nat. Mater.* **2019**, *18*, 1112.
(31) Bazylewski, P.; Divigalpitiya, R.; Fanchini, G. In situ Raman spectroscopy distinguishes between reversible and irreversible thiol modifications in l-cysteine. *RSC Adv.* **2017**, *7*, 2964−2970.
(32) Zhang, J.; Sun, X.; Wu, J. Heavy Metal Ion Detection Platforms Based on a Glutathione Probe: A Mini Review. *Appl. Sci.* **2019**, *9*, No. 489.
(33) Muthivhi, R.; Parani, S.; May, B.; Oluwafemi, O. S. Green synthesis of gelatin-noble metal polymer nanocomposites for sensing of Hg^{2+} ions in aqueous media. *Nano-Struct. Nano-Objects* **2018**, *13*, 132−138.
(34) Eda, G.; Fanchini, G.; Chhowalla, M. Large-area ultrathin films of reduced graphene oxide as a transparent and flexible electronic material. *Nat. Nanotechnol.* **2008**, *3*, 270−274.
(35) Van Middelkoop, S.; Cen, A.; Bauld, R.; Fanchini, G. In-line chemiresistors based on multilayer graphene for cadmium dication sensing in water. *FlatChem* **2019**, *17*, No. 100118.

DOI: 10.1021/acsomega.9b03246
ACS Omega 2020, 5, 643−649